

# Measurement of $\Upsilon$ Production for $p + p$ and $p + d$ Interactions at 800 GeV/c

L.Y. Zhu,<sup>6</sup> P.E. Reimer,<sup>2,7</sup> B.A. Mueller,<sup>2</sup> T.C. Awes,<sup>10</sup> M.L. Brooks,<sup>7</sup> C.N. Brown,<sup>3</sup> J.D. Bush,<sup>1</sup>  
 T.A. Carey,<sup>7</sup> T.H. Chang,<sup>9</sup> W.E. Cooper,<sup>3</sup> C.A. Gagliardi,<sup>11</sup> G.T. Garvey,<sup>7</sup> D.F. Geesaman,<sup>2</sup>  
 E.A. Hawker,<sup>11</sup> X.C. He,<sup>4</sup> D.E. Howell,<sup>6</sup> L.D. Isenhower,<sup>1</sup> D.M. Kaplan,<sup>5</sup> S.B. Kaufman,<sup>2</sup>  
 S.A. Klinksiak,<sup>8</sup> D.D. Koetke,<sup>12</sup> D.M. Lee,<sup>7</sup> W.M. Lee,<sup>3,4</sup> M.J. Leitch,<sup>7</sup> N. Makins,<sup>2,6</sup>  
 P.L. McGaughey,<sup>7</sup> J.M. Moss,<sup>7</sup> P.M. Nord,<sup>12</sup> V. Papavassiliou,<sup>9</sup> B.K. Park,<sup>7</sup> G. Petitt,<sup>4</sup> J.C. Peng,<sup>6,7</sup>  
 M.E. Sadler,<sup>1</sup> W.E. Sondheim,<sup>7</sup> P.W. Stankus,<sup>10</sup> T.N. Thompson,<sup>7</sup> R.S. Towell,<sup>1</sup> R.E. Tribble,<sup>11</sup>  
 M.A. Vasiliev,<sup>11</sup> J.C. Webb,<sup>9</sup> J.L. Willis,<sup>1</sup> P. Winter,<sup>2</sup> D.K. Wise,<sup>1</sup> Y. Yin,<sup>6</sup> and G.R. Young<sup>10</sup>

(FNAL E866/NuSea Collaboration)

<sup>1</sup>Abilene Christian University, Abilene, TX 79699

<sup>2</sup>Physics Division, Argonne National Laboratory, Argonne, IL 60439

<sup>3</sup>Fermi National Accelerator Laboratory, Batavia, IL 60510

<sup>4</sup>Georgia State University, Atlanta, GA 30303

<sup>5</sup>Illinois Institute of Technology, Chicago, IL 60616

<sup>6</sup>University of Illinois at Urbana-Champaign, Urbana, IL 61801

<sup>7</sup>Los Alamos National Laboratory, Los Alamos, NM 87545

<sup>8</sup>University of New Mexico, Albuquerque, NM 87131

<sup>9</sup>New Mexico State University, Las Cruces, NM 88003

<sup>10</sup>Oak Ridge National Laboratory, Oak Ridge, TN 37831

<sup>11</sup>Texas A&M University, College Station, TX 77843

<sup>12</sup>Valparaiso University, Valparaiso, IN 46383

(Dated: February 2, 2008)

We report a high statistics measurement of  $\Upsilon$  production with an 800 GeV/c proton beam on hydrogen and deuterium targets. The dominance of the gluon-gluon fusion process for  $\Upsilon$  production at this energy implies that the cross section ratio,  $\sigma(p + d \rightarrow \Upsilon)/2\sigma(p + p \rightarrow \Upsilon)$ , is sensitive to the gluon content in the neutron relative to that in the proton. Over the kinematic region  $0 < x_F < 0.6$ , this ratio is found to be consistent with unity, in striking contrast to the behavior of the Drell-Yan cross section ratio  $\sigma(p + d)_{DY}/2\sigma(p + p)_{DY}$ . This result shows that the gluon distributions in the proton and neutron are very similar. The  $\Upsilon$  production cross sections are also compared with the  $p + d$  and  $p + \text{Cu}$  cross sections from earlier measurements.

PACS numbers: 13.85.Qk; 14.20.Dh; 24.85.+p; 13.88.+e

In the CERN NA51 [1] and Fermilab E866/NuSea [2, 3, 4] experiments on proton-induced dimuon production, a striking difference was observed for the Drell-Yan cross sections between  $p + p$  and  $p + d$ . As the underlying mechanism for the Drell-Yan process involves quark-antiquark annihilation, this difference has been attributed to the asymmetry between the up and down sea quark distributions in the proton. From the  $\sigma(p + d)_{DY}/2\sigma(p + p)_{DY}$  ratios the Bjorken- $x$  dependence of the sea-quark  $\bar{d}/\bar{u}$  flavor asymmetry has been extracted [1, 2, 3, 4].

The Fermilab E866 dimuon experiment also recorded a large number of  $\Upsilon \rightarrow \mu^+\mu^-$  events. In this paper, we present results on the  $\Upsilon$  differential cross sections for  $p + p$  and  $p + d$  over the kinematic range  $0 < p_T < 3.5$  GeV/c and  $0 < x_F < 0.6$ . Unlike the electromagnetic Drell-Yan process, quarkonium production is a strong interaction dominated by the subprocess of gluon-gluon fusion at this beam energy [5, 6]. Therefore, the quarkonium production cross sections are primarily sensitive to the gluon distributions in the colliding hadrons. The  $\Upsilon$  production ratio,  $\sigma(p + d \rightarrow \Upsilon)/2\sigma(p + p \rightarrow \Upsilon)$ , is expected to probe the gluon content in the neutron relative to that in the proton [7]. As pointed out by Piller

and Thomas [7], charge symmetry violation at the parton level could lead to a different gluon distribution in the proton versus that in the neutron. A precise measurement of the  $\sigma(p + d \rightarrow \Upsilon)/2\sigma(p + p \rightarrow \Upsilon)$  ratios would provide a constraint on the effect of charge symmetry violation on the gluon distributions.

High statistics  $\Upsilon$  production cross sections at 800 GeV have been reported for  $p + d$  [8] and  $p + \text{Cu}$  [9]. The per-nucleon cross sections for  $p + d$  were roughly a factor of two greater than those of  $p + \text{Cu}$ . Such a difference could not be explained by the nuclear effect of  $\Upsilon$  production, which was found to be small [10]. The  $p + p$  and  $p + d$  data would shed new light on this apparent discrepancy. Moreover,  $\Upsilon$  production in the simple  $p + p$  and  $p + d$  systems provides the baseline information for future searches of possible suppression of  $\Upsilon$  production as a signature for a quark-gluon plasma in relativistic heavy-ion collisions [11, 12].

The experiment was performed at Fermilab using the upgraded Meson-East magnetic pair spectrometer. Details of the experimental setup can be found elsewhere [4, 13, 14]. A primary proton beam with up to  $2 \times 10^{12}$  protons per 20-second beam spill was incident

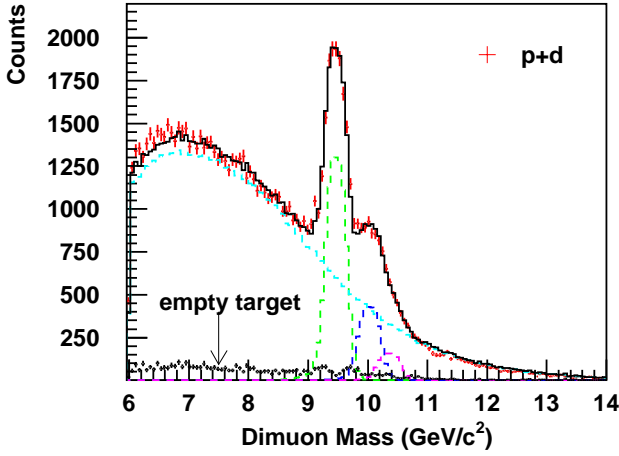


FIG. 1: (color online). Dimuon mass spectrum for  $p + d$  interactions at 800 GeV/c. Fit to the spectrum is shown as the solid curve. Contributions from the Drell-Yan continuum and  $\Upsilon$  resonances are shown as dashed curves. The luminosity weighted spectrum from the empty-target measurements is also shown.

upon one of three identical 50.8-cm long cylindrical stainless steel target flasks containing either liquid hydrogen, liquid deuterium, or vacuum. A copper beam dump located inside the second dipole magnet absorbed the protons that passed through the target. Downstream of the beam dump was a 13.4 interaction-length absorber wall of copper, carbon and polyethylene that completely filled the aperture of the magnet. This absorber wall removed hadrons produced in the target and the beam dump.

The targets alternated between hydrogen and deuterium every five beam spills with a single spill collected on the empty flask at each target change. Beam intensity was monitored by secondary-emission detectors, an ion chamber, and quarter-wave RF cavities. Two scintillator telescopes viewing the targets at  $90^\circ$  monitored the luminosity, beam duty factor and data acquisition live-time. The detector system consisted of four tracking stations and a momentum analyzing magnet. The trigger required a pair of triple hodoscope coincidences having a pattern consistent with a muon pair from the target.

Tracks reconstructed in the drift chambers were extrapolated to the target using the momentum determined by the analyzing magnet. The target position was used to refine the parameters of each muon track. The resulting rms mass resolution for the  $\Upsilon$  resonances is  $\approx 250$  MeV. Monte Carlo studies show that this resolution is dominated by the finite target length and the multiple scattering of muons in the absorber. Figure 1 shows the dimuon mass spectra for the high-mass data collected with the deuterium target. The high-mass data set contains approximately 20,000  $\Upsilon$  events.

To extract the yields of the  $\Upsilon$  resonances, the contributions of the Drell-Yan continuum under the  $\Upsilon$  resonances

TABLE I: Product of the  $\Upsilon$  production cross section per nucleon and the  $\Upsilon \rightarrow \mu^+\mu^-$  branching ratio ( $B$ ) for  $p + d$  and  $p + p$  interactions at 800 GeV/c. The uncertainties are statistical only. The values of  $p_0$  are also listed.

$x_F$	$B \cdot d\sigma/dx_F(\text{pb})$ for $pd \rightarrow \mu^+\mu^- X$		
	$\Upsilon(1S)$	$\Upsilon(2S)$	$\Upsilon(3S)$
0.05	$3.246 \pm 0.119$	$0.969 \pm 0.081$	$0.529 \pm 0.064$
0.15	$2.963 \pm 0.080$	$0.863 \pm 0.054$	$0.250 \pm 0.042$
0.25	$1.934 \pm 0.059$	$0.666 \pm 0.041$	$0.224 \pm 0.031$
0.35	$1.253 \pm 0.043$	$0.453 \pm 0.032$	$0.177 \pm 0.026$
0.45	$0.620 \pm 0.030$	$0.240 \pm 0.024$	$0.075 \pm 0.020$
0.55	$0.227 \pm 0.021$	$0.095 \pm 0.018$	$0.046 \pm 0.014$
$p_T(\text{GeV}/c)$	$B \cdot d\sigma/dp_T^2(\text{pb}/\text{GeV}^2/c^2)$ for $pd \rightarrow \mu^+\mu^- X$		
	$\Upsilon(1S)$	$\Upsilon(2S)$	$\Upsilon(3S)$
0.25	$0.8648 \pm 0.0381$	$0.3921 \pm 0.0307$	$0.1063 \pm 0.0246$
0.75	$0.6347 \pm 0.0184$	$0.2264 \pm 0.0143$	$0.0804 \pm 0.0116$
1.25	$0.3996 \pm 0.0112$	$0.1225 \pm 0.0083$	$0.0563 \pm 0.0064$
1.75	$0.1968 \pm 0.0070$	$0.0610 \pm 0.0049$	$0.0228 \pm 0.0037$
2.25	$0.0964 \pm 0.0043$	$0.0281 \pm 0.0029$	$0.0114 \pm 0.0022$
2.75	$0.0416 \pm 0.0027$	$0.0111 \pm 0.0017$	$0.0050 \pm 0.0014$
3.25	$0.0191 \pm 0.0017$	$0.0029 \pm 0.0011$	$0.0030 \pm 0.0009$
$p_0(\text{GeV}/c)$	$3.39 \pm 0.04$	$3.06 \pm 0.07$	$3.36 \pm 0.17$
$x_F$	$B \cdot d\sigma/dx_F(\text{pb})$ for $pp \rightarrow \mu^+\mu^- X$		
	$\Upsilon(1S)$	$\Upsilon(2S)$	$\Upsilon(3S)$
0.05	$3.435 \pm 0.182$	$0.946 \pm 0.119$	$0.454 \pm 0.092$
0.15	$3.025 \pm 0.119$	$0.731 \pm 0.079$	$0.408 \pm 0.065$
0.25	$1.946 \pm 0.086$	$0.601 \pm 0.061$	$0.292 \pm 0.051$
0.35	$1.397 \pm 0.065$	$0.334 \pm 0.046$	$0.181 \pm 0.037$
0.45	$0.652 \pm 0.046$	$0.214 \pm 0.035$	$0.066 \pm 0.028$
0.55	$0.253 \pm 0.031$	$0.098 \pm 0.024$	$0.038 \pm 0.019$
$p_T(\text{GeV}/c)$	$B \cdot d\sigma/dp_T^2(\text{pb}/\text{GeV}^2/c^2)$ for $pp \rightarrow \mu^+\mu^- X$		
	$\Upsilon(1S)$	$\Upsilon(2S)$	$\Upsilon(3S)$
0.25	$0.8754 \pm 0.0576$	$0.3381 \pm 0.0448$	$0.1102 \pm 0.0374$
0.75	$0.6482 \pm 0.0276$	$0.2057 \pm 0.0218$	$0.0662 \pm 0.0164$
1.25	$0.3934 \pm 0.0161$	$0.0972 \pm 0.0119$	$0.0594 \pm 0.0098$
1.75	$0.2167 \pm 0.0107$	$0.0467 \pm 0.0069$	$0.0334 \pm 0.0058$
2.25	$0.1008 \pm 0.0064$	$0.0236 \pm 0.0042$	$0.0188 \pm 0.0035$
2.75	$0.0437 \pm 0.0040$	$0.0146 \pm 0.0027$	$0.0013 \pm 0.0012$
3.25	$0.0232 \pm 0.0027$	$0.0063 \pm 0.0019$	$0.0035 \pm 0.0021$
$p_0(\text{GeV}/c)$	$3.47 \pm 0.05$	$3.20 \pm 0.15$	$3.22 \pm 0.18$

need to be determined and subtracted. Monte Carlo simulations for Drell-Yan events using next-to-leading order calculations and the MRS98 [15] parton distributions, which reproduce the  $\bar{d}/\bar{u}$  asymmetry observed in the E866 Drell-Yan data [4, 14], were carried out. The line shapes of the three  $\Upsilon$  resonances were also calculated using Monte Carlo. For each  $x_F$  and  $p_T$  bin, the normalization factors for the Drell-Yan and the  $\Upsilon$  resonances were adjusted to fit the data. Contributions of

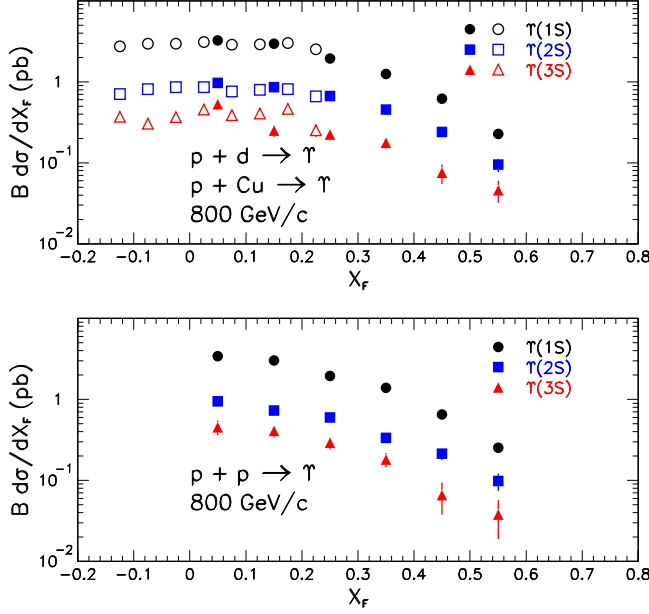


FIG. 2: (color online). Upper panel:  $B \cdot d\sigma/dx_F$  (per target nucleon) for  $\Upsilon(1S)$ ,  $\Upsilon(2S)$ , and  $\Upsilon(3S)$  production cross sections for  $p + d$  at 800 GeV/c. The E605 data [9] for  $p + Cu$  are also shown as open symbols. Lower panel:  $B \cdot d\sigma/dx_F$  for  $\Upsilon(1S)$ ,  $\Upsilon(2S)$ , and  $\Upsilon(3S)$  production for  $p + p$  at 800 GeV/c.

dimuon events from the stainless steel target flask were subtracted using data obtained with the empty-target measurements. The Drell-Yan normalization factors were found to be consistent with unity, showing good agreements between the data and the Monte Carlo simulation. The dimuon mass spectra are well described by the sum of the various contributions considered in the analysis, as illustrated in Fig. 1 for the  $p + d$  data. The mass spectra for various  $x_F$  and  $p_T$  bins are also well described using this fitting procedure.

The values of  $Bd\sigma/dx_F$  per target nucleon for the three  $\Upsilon$  resonances in  $p + p$  and  $p + d$  collisions are shown in Fig. 2 and listed in Tab. I ( $B$  is the branching ratio for  $\Upsilon \rightarrow \mu^+\mu^-$  decay). The  $d\sigma/dx_F$  differential cross sections are obtained by integrating over  $p_T$  using a  $p_T$  distribution which best fits the data. A  $\pm 6.5\%$  overall normalization uncertainty, common to both the  $p + p$  and  $p + d$  cross sections, is associated with the determination of the beam intensity [4]. Other systematic errors due to the uncertainty of the magnetic fields of the spectrometer and the hodoscope efficiency are estimated to be  $\pm 3\%$ . Existing E605 data [9] for  $p + Cu$  collision covering the kinematic range  $-0.15 < x_F < 0.25$  are also shown for comparison. The good agreement between the E866  $p + d$  and the E605  $p + Cu$  data is consistent with the  $A$ -dependence measurement performed by E772 [10], which showed that the cross section is proportional to  $A^\alpha$  with  $\alpha \approx 0.962$ . Figure 2 also shows that the relative yields for producing the  $\Upsilon(1S)$ ,  $\Upsilon(2S)$ , and  $\Upsilon(3S)$  resonances

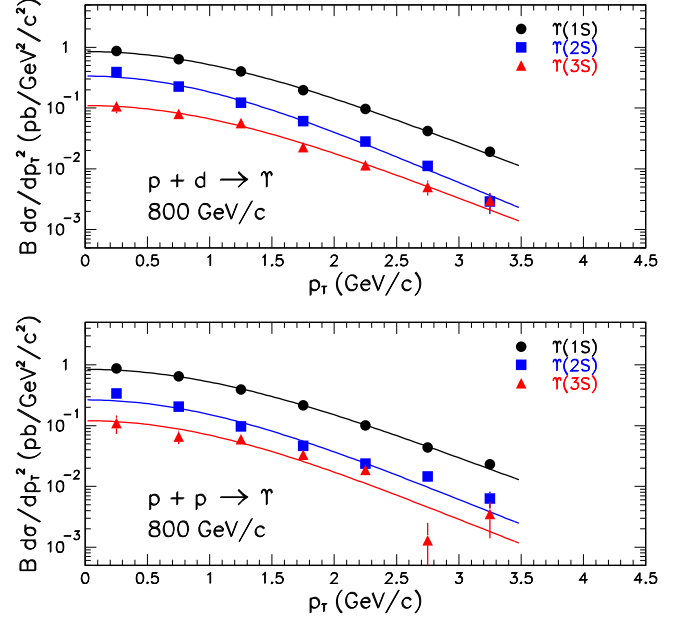


FIG. 3: (color online).  $B \cdot d\sigma/dp_T^2$  (per target nucleon) for  $\Upsilon$  production cross sections for  $p + d$  and  $p + p$  from the E866 measurement. The curves correspond to fits described in the text.

are very similar for  $p + d$  and  $p + Cu$ , consistent with no significant nuclear dependences for these relative yields. From this experiment, the ratios  $B\sigma(\Upsilon(2S))/B\sigma(\Upsilon(1S))$  and  $B\sigma(\Upsilon(3S))/B\sigma(\Upsilon(1S))$  over  $0 \leq x_F \leq 0.6$  are determined as  $0.321 \pm 0.012$  and  $0.127 \pm 0.009$  for  $p + d$ .

The  $p_T$  dependences of the  $\Upsilon(1S)$ ,  $\Upsilon(2S)$  and  $\Upsilon(3S)$  cross sections are listed in Tab. I and shown in Fig. 3 for  $p + d$  and  $p + p$ . The  $d\sigma/dp_T^2$  differential cross sections are obtained by integrating over the  $-1 < x_F < 1$  range using a parametrization which best describes the data. These  $p_T$  distributions are fitted with the parametrization  $d\sigma/dp_T^2 = c(1 + p_T^2/p_0^2)^{-6}$  [17] and the results of the fits are shown in Fig. 3. The values of  $p_0$ , listed in Tab. I, are somewhat lower than the E605 result [9] where  $p_0 = 3.7$  GeV/c was obtained.

Figure 4 compares the  $\Upsilon(1S)$  production cross section at 800 GeV/c measured for  $p + d$  in E866 and E772 [8], and for  $p + Cu$  in E605 [9]. The E772 cross sections are roughly a factor of two greater than those of E866 and E605. Moreover, the shape of the E772 differential cross sections has a steeper fall-off as  $x_F$  increases. To shed some light on this apparent discrepancy, calculations for  $d\sigma/dx_F$  using the color-evaporation model (CEM) [20] have been performed. The CEM was known to be capable of describing the  $x_F$  and energy dependences of quarkonium production successfully [12, 21]. The probability for forming a given quarkonium state is treated as a parameter in this model. As shown in Fig. 4, the  $x_F$  dependences of both the E866 and the E605 data are well described by calculations using two different parton

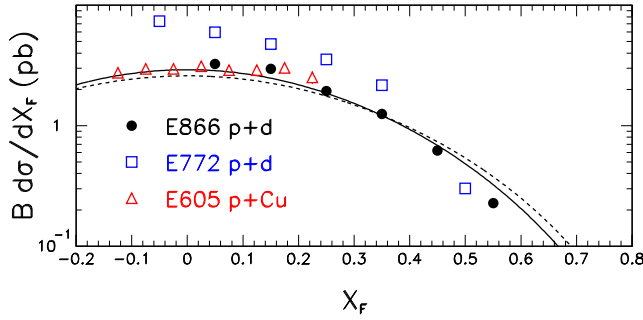


FIG. 4: (color online). Comparison of the  $\Upsilon(1S)$  production cross sections between E866, E772 [8], and E605 [9]. The solid and dashed curves correspond to the color-evaporation model calculations using the CTEQ4M and CTEQ5L parton distribution functions, respectively. The absolute normalizations of the calculations are adjusted to fit the E866 data.

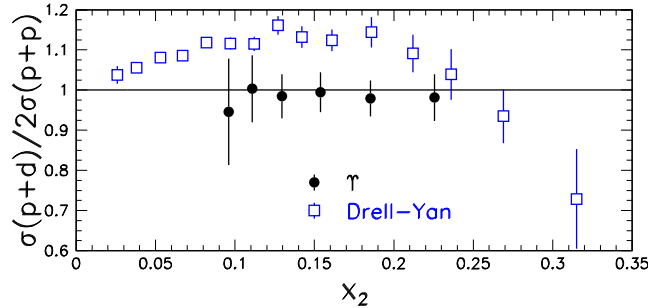


FIG. 5: (color online). The E866  $\sigma(p+d)/2\sigma(p+p)$  cross section ratios for  $\Upsilon$  resonances as a function of  $x_2$ . The corresponding ratios for the E866 Drell-Yan cross sections [4] are also shown. The error bars are statistical only.

distribution functions. In contrast, the E772 data show a steeper  $x_F$  dependence than the prediction of the CEM. While the origin of the discrepancy between the E866 and the earlier E772 results is not understood, the good agreement between the data and the CEM calculation tends to favor the E866 results.

The  $\sigma(p+d)/2\sigma(p+p)$  ratios for  $\Upsilon(1S+2S+3S)$  production are shown in Fig. 5 as a function of  $x_2$ , the Bjorken- $x$  of the target parton. Most of the systematic errors cancel for these ratios, with a remaining  $\approx 1\%$  error from the rate dependence and target compositions [4]. Figure 5 shows that these ratios are consistent with unity, in striking contrast to the corresponding values [4] for the Drell-Yan process, also shown in Fig. 5. The difference between the Drell-Yan and the  $\Upsilon$  cross section ratios clearly reflect the different underlying mechanisms in these two processes. The Drell-Yan process, dominated by the  $u-\bar{u}$  annihilation subprocess, leads to the relation  $\sigma(p+d)_{DY}/2\sigma(p+p)_{DY} \approx \frac{1}{2}(1 + \bar{u}_n(x_2)/\bar{u}_p(x_2)) = \frac{1}{2}(1 + \bar{d}_p(x_2)/\bar{u}_p(x_2))$ , where  $\bar{q}_{p,n}$  refers to the  $\bar{q}$  distribution in the proton and neutron, respec-

tively. For  $\Upsilon$  production, the dominance of the gluon-gluon fusion subprocess at this beam energy implies that  $\sigma(p+d \rightarrow \Upsilon)/2\sigma(p+p \rightarrow \Upsilon) \approx \frac{1}{2}(1 + g_n(x_2)/g_p(x_2))$ . Figure 5 shows that the gluon distributions in the proton ( $g_p$ ) and neutron ( $g_n$ ) are very similar over the  $x_2$  range  $0.09 < x_2 < 0.25$ . The overall  $\sigma(p+d \rightarrow \Upsilon)/2\sigma(p+p \rightarrow \Upsilon)$  ratio, integrated over the measured kinematic range, is  $0.984 \pm 0.026(\text{stat.}) \pm 0.01(\text{syst.})$ . These results are consistent with no charge symmetry breaking effect in the gluon distributions.

In summary, we report the measurement of  $\Upsilon$  production for  $p+p$  and  $p+d$  interactions at 800 GeV/c. This measurement allows a first determination of the  $\sigma(p+d \rightarrow \Upsilon)/2\sigma(p+p \rightarrow \Upsilon)$  ratio, which complements the previous measurement of the corresponding Drell-Yan ratio. The  $\Upsilon$  data indicate that the gluon distributions in the proton and neutron are very similar. A comparison of the  $p+d$  data with the previous E605  $p+Cu$  data shows no significant nuclear effects for  $\Upsilon$  production in the kinematic region near  $x_F \sim 0$ , consistent with the previous E772 nuclear-dependence measurement.

This work was supported in part by the U.S. Department of Energy and the National Science Foundation.

- 
- [1] A. Baldit *et al.*, Phys. Lett. B **332**, 244 (1994).
  - [2] Fermilab E866 Collaboration, E.A. Hawker *et al.*, Phys. Rev. Lett. **80**, 3715 (1998).
  - [3] Fermilab E866 Collaboration, J.C. Peng *et al.*, Phys. Rev. D **58**, 092004 (1998).
  - [4] Fermilab E866 Collaboration, R.S. Towell *et al.*, Phys. Rev. D **64**, 052002 (2001).
  - [5] J.C. Peng, D.M. Jansen, and Y.C. Chen, Phys. Lett. B **344**, 1 (1995).
  - [6] R. Vogt, Phys. Rep. **310**, 197 (1999).
  - [7] G. Piller and A.W. Thomas, Z. Phys. C **70**, 661 (1996).
  - [8] Fermilab E772 Collaboration, P.L. McGaughey *et al.*, Phys. Rev. D **50**, 3038 (1994).
  - [9] Fermilab E605 Collaboration, G. Moreno *et al.*, Phys. Rev. D **43**, 2815 (1991).
  - [10] Fermilab E772 Collaboration, D.M. Alde *et al.*, Phys. Rev. Lett. **66**, 2285 (1991).
  - [11] F. Karsch, M.T. Mehr, and H. Satz, Z. Phys. C **37**, 617 (1988).
  - [12] M. Bedjidian *et al.* hep-ph/0311048.
  - [13] Fermilab E866 Collaboration, C.N. Brown *et al.*, Phys. Rev. Lett. **86**, 2529 (2001).
  - [14] R.S. Towell, Ph.D thesis, University of Texas, 1999, nucl-ex/0102012.
  - [15] A.D. Martin *et al.*, Eur. Phys. J. C **4**, 463 (1998).
  - [16] H.L. Lai *et al.*, Eur. Phys. J. C **12**, 375 (2000).
  - [17] D.M. Kaplan *et al.*, Phys. Rev. Lett. **40**, 435 (1978).
  - [18] D.E. Groom *et al.*, Eur. Phys. J. C **15**, 1 (2000).
  - [19] M.C. Abreu *et al.*, Phys. Lett. B **438**, 35 (1998).
  - [20] H. Fritzsch, Phys. Lett. B **67**, 217 (1977).
  - [21] G.A. Schuler and R. Vogt, Phys. Lett. B **387**, 181 (1996).